Inelastic scattering and sticking of hydrogen molecules at adsorbed rare-gas overlayers

C.M. Hedenäs* and M. Persson

Institute of Theoretical Physics, Chalmers University of Technology, S-412 96 Göteborg, Sweden
(Received 7 November 1991)

A method for treating strongly inelastic scattering of light atoms and molecules from rare-gas overlayers with close-coupling wave packets is proposed. The multiphonon distributions for the excitation of the rare-gas atoms, treated as Einstein oscillators, are calculated in one and two dimensions for a single excited oscillator as well as for in-phase excitation of the overlayer. Strong inelasticity and deviations from Poisson distributions are found especially for the scattering of H_2 from Ar, less from Kr or Xe. We also show that this method is able to handle the dynamics of sticking and trapping on these overlayers.

I. INTRODUCTION

The study of inelastic scattering of atoms and molecules from surfaces is one of the central fields in surface science. Recent advances in thermal molecular-beam scattering from well-characterized surfaces have made it possible to make detailed studies of the mechanisms behind gas-surface energy transfer and sticking of atoms and molecules on surfaces. Even for a nonreactive systems several different issues remain to be settled concerning these mechanisms, like the relative importance of electron-hole pairs and phonons at metal surfaces, the role of rotations and vibrations of the incident particle, and the relative importance of inelastic scattering and surface corrugation on sticking. The theoretical description of these processes also poses a many-body scattering problem of fundamental interest in its own right.

The physisorption of atoms and molecules on surfaces is one of simplest classes of systems to describe theoretically. The physisorption interaction is believed to be electronically adiabatic in most cases, which means that the substrate phonons are the dominant channels for energy transfer. A quantum-mechanical description of the energy transfer to phonons has been found to be imperative in many cases for light atoms and molecules in this class of systems. The importance of quantum effects has for instance been demonstrated for the sticking of Ne on Ru(100) (Ref. 1) and also for hydrogen molecules on Cu(100).[2] These two cases, as well as the scattering of thermal He beams from clean surfaces, are examples where the inelasticity is weak and where the energy transfer is dominated by one-phonon processes at low incident energies. The one-phonon regime of inelastic scattering can be handled theoretically by the distorted-wave Born approximation[3] while in the situation of strong inelastic scattering the theoretical description is much less developed.

A most interesting class of surfaces where strongly inelastic scattering can be studied in the quantum regime both theoretically and experimentally is provided by the ordered rare-gas overlayers on metal surfaces. The He-

beam scattering studies from ordered Xe overlayers on Cu(100) by Mason and Williams[4] have shown that the low-energy adsorbate phonons in these systems can be multiply excited. Such multiple excitations have more recently also been observed on Ar, Kr, and Xe monolayers on Ag(111),[5,6] and Kr and Xe monolayers on Pt(111).[7,8] In these later experimental studies the Einstein-oscillator character of the adsorbate modes were demonstrated from measurements of their dispersion with momentum transfer parallel to the surface. Another most attractive feature for the theoretical modeling of this class of systems, besides the simple nature of the surface vibrational modes, is that the particle-surface interaction is known from measured atom or molecule rare-gas potentials and the van der Waal particle–metal-surface interaction. Inelastic scattering of He from Xe overlayers has been studied theoretically by Kosloff and Cerjan.[9] Their mean-field treatment of the atom-phonon interaction gives, however, a poor description of the large inelastic effects in this system.

We have developed a fully quantum-mechanical method that is able to handle the effects of both strong inelasticity and surface corrugation on the energy transfer and sticking. The method is based on the approximation that multiphonon excitations can occur only at a single site in the inelastic scattering of a particle from an ordered lattice of Einstein oscillators and solving the resulting equations using a pseudospectral technique for propagating close-coupled wave packets. This approximation is developed within the framework of a formally exact multiphonon expansion introduced by Stiles, Wilkins, and Persson.[10] The Einstein-oscillator character of the phonons and the localized particle-surface interaction gives the physical motivation for the approximation. We have also compared our results with an in-phase multiphonon approximation where all Einstein-oscillator phonons are excited in phase. However, this approximation will not describe sticking but only temporary trapping since the energy transferred to the phonons will be transferred back to the trapped particle.

This quantum-mechanical method has been applied to

the scattering and sticking of a hydrogen molecule at Ar, Kr, and Xe overlayers on Ag(111). We have chosen to study a hydrogen molecule instead of a He atom since the well depth of the molecule-surface interaction is sufficiently deep to also make experimental studies of the sticking practical. The calculations of multiphonon excitations and trapping and sticking coefficients have mostly been performed at a single energy, and we have restricted the motion of the molecule to be two dimensional and in the in-phase multiphonon approximation we have also considered the further restriction that the motion should be one dimensional. All calculations are done at normal incidence and at zero substrate temperature but can readily be done at off-normal incidence and nonzero temperatures.

The overall behavior of the calculated multiphonon loss distributions can be understood semiquantitatively from a forced-oscillator model combined with the results from a simple Baule model for the energy transfer. In particular we find that our calculated loss distributions are close to a Poisson distribution for H_2 on a heavy rare-gas atom overlayer like Xe, while large deviations are found on Ar where the inelasticity is stronger due to the larger mass ratio. A result that should be of direct experimental interest, and that we plan to calculate in the future, is the calculation of the full momentum-resolved multiphonon loss distributions, which can be directly compared with measured distributions. In the single-site approximation we find that the calculated sticking coefficient is close to the calculated initial trapping coefficient in the in-phase approximation even in the one-dimensional calculation. This result can be understood from the fact that the energy transfer back to the trapped particle is slow compared to the time it takes for the particle to move away from the excited atom. A most important result in the single-site approximation is that the calculated initial trapping coefficient into states with a perpendicular energy less than zero is much larger than the sticking coefficient into states with energy less than zero. This is a combined effect of strong corrugation and inelasticity, which makes it possible for the particle to scatter into states with large momentum parallel to the surface at normal incidence. This is an important effect for these systems, which also should be of direct experimental interest and is not expected for systems with weak inelasticity and surface corrugation. For instance, in the case of sticking of hydrogen molecules on Cu(100) the trapping into such states is appreciable only at large angles of incidence.

The remaining part of this paper is organized as follows. In Sec. II we first define the particle-surface scattering problem by introducing its Hamiltonian while the details of the molecule-surface interaction is postponed to the last subsection. The equations of motion obtained in the single-site and in-phase multiphonon approximations together with a detailed presentation of their solution in terms of close-coupled wave packets are also given in this section. In Sec. III we give and discuss the results for the multiphonon loss distributions and the sticking of H_2 at the Ar, Kr, and Xe overlayers on Ag(111). Finally, in Sec. IV we summarize and conclude.

II. THEORY

A. Hamiltonian

As already mentioned, we want to treat the inelastic scattering and sticking of a hydrogen molecule on a metal surface covered with a monolayer of noble-gas atoms. Inelastic He scattering studies have shown that the energy transfer to the adsorbate layer is dominated by low-energy adsorbate modes polarized normal to the surface. These modes show no dispersion with the momentum transfer, and the observed energies of the multiple losses are well described in the harmonic approximation. These facts are the main reasons why we only include these Einstein-oscillator phonons in our model. The molecule is treated as a structureless particle with no internal vibrations or rotations. The neglect of internal vibrations is obviously justified in our case since the vibrational energy is very large compared to the considered energy scale of the molecule-surface interaction. Even the rotational spacing of about 44 meV $(j = 0 \rightarrow 2)$ of the hydrogen molecule is relatively large compared to this energy scale. This fact combined with the small anisotropy of the hydrogen–rare-gas atom potentials justifies the neglect of the rotations in this context.

The Hamiltonian H of the molecule-phonon system can be written as a sum of a molecule part, H_p, a lattice part, H_{latt}, and an interaction part, V_{int},

$$H = H_p + H_{latt} + V_{int}(\mathbf{r}, \{u_z(\mathbf{R})\}). \qquad (1)$$

Here $\mathbf{r}$ is the position of the center of mass of the molecule and $u_z(\mathbf{R})$ is the displacement of the noble-gas atoms from its equilibrium positions, $\mathbf{R}$. The rigid surface potential $V_0(\mathbf{r})$ is included in the particle part of the Hamiltonian,

$$H_p = \frac{\mathbf{p}^2}{2m_p} + V_0(\mathbf{r}), \qquad (2)$$

where m_p is the particle mass. The Hamiltonian corresponding to the undisturbed two-dimensional lattice of Einstein-oscillator modes can be written

$$H_{latt} = \sum_{\mathbf{R}} \omega_E \, [b(\mathbf{R})^{\dagger} b(\mathbf{R}) + \tfrac{1}{2}], \qquad (3)$$

where $b(\mathbf{R})^{\dagger}$ creates an Einstein-oscillator phonon at site $\mathbf{R}$. The Einstein-oscillator frequencies ω_E are listed together with the lattice constants in Table I for the considered rare-gas overlayers. Note that we use units where $\hbar = 1$.

The total interaction potential $V(\mathbf{r}, \{u_z(\mathbf{R})\})$ between

TABLE I. The energies of the Einstein oscillators and the lattice constants for the different rare-gas overlayers.

	Phonon energy $\hbar\omega_E$ (meV)	Lattice parameter (a_0)
Ar	3.7	7.18
Kr	2.9	7.56
Xe	2.8	8.31

the molecule and the surface is expanded in the displacements $u_z(\mathbf{R})$ of the noble-gas atoms perpendicular to the surface. The zero-order term is $V_0(\mathbf{r})$, which is included in H_p; the other terms are included in V_{int}. In our calculations we have found that the low energy of the Einstein-oscillator modes together with the rather strong molecule-surface interaction potential makes it necessary to go beyond a linear coupling model, and to include also the second-order term in the expansion of $V(\mathbf{r}, \{u_z(\mathbf{R})\})$ in $u_z(\mathbf{R})$. The interaction term V_{int} can then be written using the expansion

$$u_z(\mathbf{R}) = \frac{1}{\sqrt{2m_a\omega_E}} [b(\mathbf{R}) + b(\mathbf{R})^\dagger] \qquad (4)$$

as

$$V_{int}(\mathbf{r}, \{u_z(\mathbf{R})\}) = \sum_{\mathbf{R}} g(\mathbf{r}, \mathbf{R})[b(\mathbf{R}) + b(\mathbf{R})^\dagger]$$
$$+ \sum_{\mathbf{R},\mathbf{R'}} d(\mathbf{r}, \mathbf{R}, \mathbf{R'})[b(\mathbf{R}) + b(\mathbf{R})^\dagger]$$
$$\times [b(\mathbf{R'}) + b(\mathbf{R'})^\dagger], \qquad (5)$$

with

$$g(\mathbf{r}, \mathbf{R}) = \frac{1}{\sqrt{2m_a\omega_E}} \frac{\partial V}{\partial u_z(\mathbf{R})} \qquad (6)$$

and

$$d(\mathbf{r}, \mathbf{R}, \mathbf{R'}) = \frac{1}{4m_a\omega_E} \frac{\partial^2 V}{\partial u_z(\mathbf{R})\partial u_z(\mathbf{R'})}, \qquad (7)$$

where m_a is the noble-gas-atom mass. The explicit form of the rigid surface potential $V_0(\mathbf{r})$ and the linear and second-order coupling terms $g(\mathbf{r}, \mathbf{R})$ and $d(\mathbf{r}, \mathbf{R}, \mathbf{R'})$ for the scattering of a hydrogen molecule from the Ar, Kr, and Xe overlayers will be discussed in a later section.

B. Single-site multiphonon approximation

The inelastic particle-surface scattering problem posed by the Hamiltonian in (1) is a formidable many-body problem despite the simple nature of the adsorbate vibrational modes. This problem is attacked within a theoretical framework based on a formally exact multiphonon expansion developed by Stiles, Wilkins, and Persson.[10] The particle-phonon interaction is of very short range, and in most situations limited to a single adsorbate atom. Our proposed approximation is based on the assumption that multiple phonon excitations are created only on a single site in the initial collision. For comparison we also consider the other extreme case where all the Einstein modes are excited in phase. The proposed approximations are developed for zero substrate temperature but can be generalized to nonzero temperatures.

The amplitudes corresponding to the multiphonon excitations are characterized by the number of phonons excited at each site $\mathbf{R}$, $\{n(\mathbf{R})\}$. We define the amplitude for the hydrogen molecule to be at $\mathbf{r}$ when the noble-gas-atom oscillators are in the state $\{n(\mathbf{R})\}$,

$$\psi(\mathbf{r}, \{n(\mathbf{R})\}, t) = \frac{\left\langle \prod_{\mathbf{R}} \hat{b}(\mathbf{R}, t)^{n(\mathbf{R})} \hat{\psi}(\mathbf{r}, t) \right\rangle}{\sqrt{\prod_{\mathbf{R}} n(\mathbf{R})!}}, \qquad (8)$$

where the angular brackets denote a thermal average. The time evolution of the amplitude operator

$$\hat{\psi}(\mathbf{r}, t) = e^{iH_{latt}t}\langle \mathbf{r}|e^{-iHt}|\chi(0)\rangle \qquad (9)$$

is governed by[10]

$$i\frac{\partial}{\partial t}\hat{\psi}(\mathbf{r}, t) = \left[H_p + \hat{V}_{int}(\mathbf{r}, t)\right]\hat{\psi}(\mathbf{r}, t). \qquad (10)$$

Here $\chi(0)$ is the initial particle wave function, and operators with a caret are defined by

$$\hat{O}(t) = e^{iH_{latt}t}Oe^{-iH_{latt}t}. \qquad (11)$$

Taking the time derivative of ψ in (8) and inserting the equation for the amplitudes (10) and keeping for the moment only the first-order terms in the particle-phonon interaction (5), we arrive at the following coupled set of equations for the multiphonon amplitudes $\psi(\mathbf{r}, \{n(\mathbf{R})\}, t)$,

$$i\frac{\partial}{\partial t}\psi(\mathbf{r}, \{n(\mathbf{R})\}, t) = \left(H_p + \sum_{\mathbf{R'}} n(\mathbf{R'})\omega_E\right)\psi(\mathbf{r}, \{n(\mathbf{R})\}, t)$$
$$+ \sum_{\mathbf{R'}} g(\mathbf{r}, \mathbf{R'})[\sqrt{n(\mathbf{R'})+1}\,\psi(\mathbf{r}, \{n(\mathbf{R})+\delta_{\mathbf{R},\mathbf{R'}}\}, t) + \sqrt{n(\mathbf{R'})}\,\psi(\mathbf{r}, \{n(\mathbf{R})-\delta_{\mathbf{R},\mathbf{R'}}\}, t)], \qquad (12)$$

where $\delta_{\mathbf{R},\mathbf{R'}}$ is the Kronecker symbol. The second-order terms in the interaction are too lengthy to write out, but they contain amplitudes like $\psi(\mathbf{r}, \{n(\mathbf{R}) \pm \delta_{\mathbf{R},\mathbf{R'}} \pm \delta_{\mathbf{R},\mathbf{R''}}\}, t)$. It is evident from this infinite set of coupled equations for the multiphonon amplitudes that it is necessary to introduce some physically motivated approximations. As we have already stressed, we assume that most of the excitations occur due to the first impact of the molecule on the surface, and that therefore only single-site multiphonon excitations are allowed. This approximation introduces a constraint

$$\psi(\mathbf{r}, \{n(\mathbf{R})\}, t) \equiv 0, \qquad (13)$$

if $n(\mathbf{R})n(\mathbf{R'}) \neq 0$ for some $\mathbf{R} \neq \mathbf{R'}$.

Furthermore we will make use of the periodicity of the overlayer by considering an incident particle with a wave vector $\mathbf{K}_{in}$ parallel to the surface. At zero temperature

no thermally excited phonons are present, and the initial state is

$$\psi(\mathbf{r}, \{0\}, t) \xrightarrow{t \to -\infty} \psi_{\text{initial}}(\mathbf{r}, t) \equiv \psi_{\text{in}}(z, t) \, e^{i\mathbf{K}_{\text{in}} \cdot \mathbf{r}}, \tag{14}$$

with all other initial multiphonon amplitudes being zero. The amplitudes corresponding to multiple excitations of phonons at different sites then differ from each other by a phase factor, and can be written

$$\psi(\mathbf{r}, \{n(\mathbf{R})\}, t) = e^{i\mathbf{K}_{\text{in}} \cdot \mathbf{r}} \phi_n(\mathbf{r} - \mathbf{R}, t)$$

$$\text{for } n = n(\mathbf{R}) \text{ and } n(\mathbf{R}') = 0, \quad \mathbf{R}' \neq \mathbf{R}. \tag{15}$$

The zero-phonon amplitude is independent of $\mathbf{R}$ and periodic over the adsorbate layer. A multiphonon excitation at a single site breaks the translational symmetry, and

the corresponding amplitude is not periodic over the surface. Furthermore, the periodicity of the overlayer and a pair potential description of the particle-adsorbate interaction simplifies the linear and second-order coupling terms, and makes the second-order term diagonal over the adsorbate sites,

$$g(\mathbf{r}, \mathbf{R}) = g_0(\mathbf{r} - \mathbf{R}), \tag{16}$$

$$d(\mathbf{r}, \mathbf{R}, \mathbf{R}') = d_0(\mathbf{r} - \mathbf{R}) \, \delta_{\mathbf{R}, \mathbf{R}'}. \tag{17}$$

Finally, we can collect all our results obtained in the single-site multiphonon approximation and from using the surface periodicity. If ϕ is the column vector containing the amplitudes ϕ_n, the equations of motion (12) can, after the introduction of the second-order terms in (5), be written as

$$i\frac{\partial}{\partial t}\phi(\mathbf{r}, t) = \{H_p(\mathbf{K}_{\text{in}}) + [\omega_E + 2d_0(\mathbf{r})]\tilde{N} + g_0(\mathbf{r})\tilde{M}^{(1)} + d_0(\mathbf{r})\tilde{M}^{(2)}\}\phi(\mathbf{r}, t)$$

$$+ \sum_{\mathbf{R} \neq 0} [g_0(\mathbf{r} - \mathbf{R})\tilde{A}^{(1)} + d_0(\mathbf{r} - \mathbf{R})\tilde{A}^{(2)}]\phi(\mathbf{r} - \mathbf{R}, t) . \tag{18}$$

The particle Hamiltonian is now given by

$$H_p(\mathbf{K}_{\text{in}}) = \frac{(\mathbf{p} + \mathbf{K}_{\text{in}})^2}{2m_p} + V_0(\mathbf{r}) + \sum_{\mathbf{R}} d_0(\mathbf{r} - \mathbf{R}), \tag{19}$$

and $\tilde{N}$ is a diagonal matrix that gives the number of Einstein-oscillator phonons in the multiphonon amplitudes,

$$N_{n,n'} = n \, \delta_{n,n'}. \tag{20}$$

$\tilde{M}^{(1,2)}$ and $\tilde{A}^{(1,2)}$ are the matrices introduced by the linear and quadratic coupling terms in (5) that couple the different multiphonon amplitudes,

$$M_{n,n'}^{(1)} = \sqrt{n}\,\delta_{n,n'+1} + \sqrt{n'}\,\delta_{n+1,n'}, \tag{21}$$

$$M_{n,n'}^{(2)} = \sqrt{n(n-1)}\,\delta_{n,n'+2} + \sqrt{n'(n'-1)}\,\delta_{n+2,n'}, \tag{22}$$

$$A_{n,n'}^{(1)} = \delta_{n,0}\delta_{n',1}, \tag{23}$$

$$A_{n,n'}^{(2)} = \sqrt{2}\,\delta_{n,0}\delta_{n',2}. \tag{24}$$

Note that the introduction of the second-order coupling term renormalizes the static surface potential in the particle Hamiltonian from its value in the rigid lattice situation and makes the Einstein-oscillator frequencies dependent on $\mathbf{r}$. The latter renormalization is found to be an important effect in the solution of this coupled channel problem. The set of coupled equations in (18) conserves the total probability to find the particle anywhere in space and is accordingly a unitary approximation. Note that in terms of the zero and multiphonon amplitudes this unitarity condition is given by

$$1 = \int_{\text{u.c.}} d\mathbf{r} |\phi_0(\mathbf{r}, t)|^2 + \sum_n \int d\mathbf{r} |\phi_n(\mathbf{r}, t)|^2, \tag{25}$$

where the integration of the zero-phonon probability density only takes place over the surface unit cell (u.c.).

The in-phase multiphonon approximation is obtained by forcing periodic boundary conditions on the nonzero-phonon amplitudes at the edge of a single surface unit cell and taking away the sum over different sites in (18)($\tilde{A}^{(1,2)} = 0$). This corresponds to the fact that all Einstein-oscillator phonons in the adsorbate overlayer are coherently excited with the same phase or, in another terminology, the multiple excitation of the delocalized Einstein phonon at the center of the surface Brilluoin zone.

Finally, we would like to stress that the single-site approximation is not equivalent to the approximation that we have scattering from a single Einstein oscillator in an otherwise rigid ordered overlayer. The latter situation corresponds to the fact that we only allow multiple excitations on a particular site, e.g., $\mathbf{R} = 0$, while in the single-site approximation we allow for a multiphonon excitation on any of the adsorbed atoms. The physical difference between these two approximations is subtle but it is revealed by considering the following situation. Assume that the particle is scattered by the surface corrugation without making any phonon excitation into a trapped state characterized by the fact that the energy of the normal motion is less than zero. In the single-site approximation this elastically scattered particle can excite phonons at any site, which means that the probability for the particle to move along the surface without having made any excitation decays in time. In the other approximation that probability is constant as long the particle does not interact with the site $\mathbf{R} = 0$.

C. Close-coupling wave-packet solution

The equation of motion for the multiphonon amplitudes in (18) is on a form which is well suited for the so-

lution with close-coupling wave packets.[11] This method is based on a propagation of a set of wave functions or, in this case, multiphonon amplitudes in time on a grid using a pseudospectral technique to handle the kinetic part of the particle Hamiltonian. One important advantage of this method in this case compared to standard coupled-channels techniques is that the strong surface corrugation is treated effectively in real space without introducing a large number of open and closed diffractive channels, whereas the motion of the noble-gas atoms can be described with a few multiphonon amplitudes.

The pseudospectral technique introduces automatically periodic boundary conditions at the grid boundaries. At the upper boundary of the grid we have added an optical potential in a standard manner to prevent the wave packets from being reflected against the back of the surface potential. The single-site multiphonon approximation has been implemented by having a grid with several unit cells and by also including an optical potential at the sides of the grid for the nonperiodic multiphonon amplitudes with $n > 0$, to prevent scattered parts of these amplitudes to return to the interaction region. The in-phase multiphonon approximation, on the other hand, is implemented by simply keeping the periodic boundary conditions and using a grid covering only a single unit cell. From the final amplitudes after scattering we have calculated the probability for the excitation of a certain number of phonons. This calculated probability includes also the probability absorbed by the optical potential.

We have found that if only linear coupling is included between the hydrogen molecule and the noble-gas atoms the solution converges *very* slowly in the number of channels included even in the case of weak inelasticity. When quadratic coupling is also included the convergence is rapid, and we have found that eight channels, i.e., a maximum of seven phonons are excited, is enough to describe the scattering process.

Some care is needed in the choice of the method for time propagation. In the calculations using periodic boundary conditions the split-operator scheme works nicely since it is straightforward to numerically exponentiate the Hamiltonian matrix. This scheme starts to become prohibitive for a large number of multiphonon amplitudes since the Hamiltonian matrix is nondiagonal, and has to be diagonalized at each lattice point before being exponentiated. In the case of the single-site approximation the periodicity of the zero-phonon amplitude ϕ_0 introduces coupling between its value at one point, $\phi_0(\mathbf{r}, t)$, and the one- and two-phonon amplitudes a lattice vector away from this point, $\phi_1(\mathbf{r} - \mathbf{R}, t)$ and $\phi_2(\mathbf{r} - \mathbf{R}, t)$, which makes the corresponding Hamiltonian matrix grow rapidly with the number of surface unit cells included in the calculation. This rapid growth has prevented us from exponentiating this matrix and from using the split-operator propagation scheme[12] in this case. Instead we have used the second-order differencing scheme (SOD) of Askar and Cakmak,[13] which can be implemented in a straightforward manner. Unfortunately the time step necessary for a stable propagation in this method is approximately one-twentieth of the one needed in the split time propagation scheme. The time

step also has to be shorter the more channels that are included in the calculation, due to the fact that the largest eigenvalue of the potential matrix is n dependent.

Propagation in an optical potential is no problem in the split-operator propagation scheme; it just means multiplying with $\exp(\mathrm{Im}\{V\}\Delta t)$ in each time step. The second-order difference scheme is known to be unstable in the case of an optical potential. We have circumvented this problem by including the optical potential $-iV_{\mathrm{im}}$ directly in SOD in an analogous way to the split-operator scheme. If the Hamiltonian of the system is decomposed as $H = H_0 - iV_{\mathrm{im}}$, then the Schrödinger equation can be written

$$i\frac{\partial}{\partial t}\left[e^{V_{\mathrm{im}}t}\psi(t)\right] = \left(e^{V_{\mathrm{im}}t}H_0\,e^{-V_{\mathrm{im}}t}\right)\left[e^{V_{\mathrm{im}}t}\psi(t)\right].\qquad(26)$$

Now SOD can be directly applied to this Schrödinger-like equation for the transformed wave function $e^{V_{\mathrm{im}}t}\psi(t)$ with the time-dependent Hamiltonian $e^{V_{\mathrm{im}}t}H_0\,e^{-V_{\mathrm{im}}t}$, which gives

$$\psi(t + \Delta t) = e^{-2V_{\mathrm{im}}\Delta t}\psi(t - \Delta t) - i2\Delta t e^{-V_{\mathrm{im}}\Delta t}H_0\psi(t).\qquad(27)$$

This equation amounts to contributions calculated from the wave function a time step Δt earlier multiplied by $\exp(\mathrm{Im}\{V\}\Delta t)$ just as in the split-operator scheme.

D. Molecule-surface interaction potentials

Our model for the molecule-surface interaction potential follows closely the construction of the He–rare-gas-overlayer potential developed by Sibener et al.[14] The interaction between the hydrogen molecule and the surface has two different contributions; one part from the metal surface underneath the noble-gas overlayer and one part from the noble-gas atoms. The adsorbed overlayer prevents the molecule from coming close to the metal surface and the hydrogen-metal interaction is therefore dominated by the van der Waals attraction,

$$V_{\mathrm{H_2,metal}}(z) = -\frac{C_{\mathrm{vdW}}}{(z - z_{\mathrm{vdW}})^3},\qquad(28)$$

where $C_{\mathrm{vdW}} = 0.1639$ a.u. for the silver surface. The origin for the z axis is chosen to be at the equilibrium position of the noble-gas overlayer, and the positions of the van der Waal planes, z_{vdW}, are listed in Table II for the different overlayers. The hydrogen-overlayer interaction is modeled with a sum of pair potentials,

$$V_{\mathrm{H_2,noble\ gas}}(\mathbf{r}, \{\mathbf{R}\}) = \sum_{\mathbf{R}} v(|\mathbf{r} - \mathbf{R}|).\qquad(29)$$

These pair potentials are chosen to have an exponentially repulsive part, and in the attractive part only an r^{-6} term is included:

$$v(r) = Ae^{-br} - \frac{C_6\,f_6(br)}{r^6},\qquad(30)$$

where we have followed Tang and Toennies[15] suggestion

TABLE II.   Potential parameters for the hydrogen-surface interaction.

	z_{vdW} (a_0)	C_6 (a.u.)	b (a_0)	A (a.u.)
Ar	-3.515	28.4	1.79	15.25
Kr	-3.704	40.2	1.87	46.86
Xe	-4.176	56.2	2.04	280.5

to damp the van der Waal attraction at short distances by

$$f_6(x) = 1 - \sum_{k=0}^{6} \frac{x^k}{k!} e^{-x}. \qquad (31)$$

The parameters b and C_6 agree with the corresponding parameters suggested by Tang and Toennies in their analysis of gas phase scattering data using a more sophisticated potential, while the parameter A has been adjusted to reproduce their derived well depths. All these potential parameters are listed in Table II. The attractive terms due to correlated charge fluctuations over more than two atoms have been shown to be a small effect for the interaction of He.[14] These many-body interaction terms are neglected in this work.

The total molecule-surface interaction potential is now given by

$$V(\mathbf{r}, \{\mathbf{R}\}) = V_{H_2,\text{noble gas}}(\mathbf{r}, \{\mathbf{R}\}) + V_{H_2,\text{metal}}(z). \qquad (32)$$

The rigid surface potential $V_0(\mathbf{r})$ is obtained from V by clamping the adsorbates at their equilibrium positions and the linear and quadratic coupling terms are obtained from V using (6) and (7). The resulting $V_0(\mathbf{r})$ are shown in Fig. 1 for the different rare-gas overlayers. Note that the well depths are about the same for all the different layers, while the distances from the overlayers to the potential minima increase with increasing size of the rare-gas atoms.
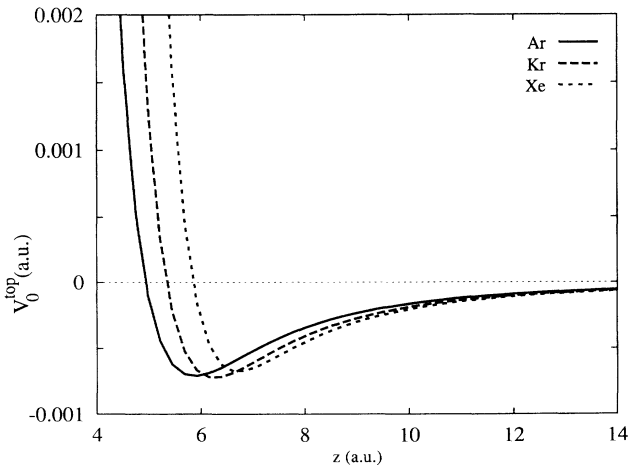

FIG. 1.   The zero-order contribution to the potential energy for a hydrogen molecule above the top of a noble-gas atom.

III. RESULTS AND DISCUSSION

In this paper we only consider normal incidence of the hydrogen molecule on the adsorbate layer and also restrict the motion to be either one dimensional or two dimensional.   In the one-dimensional calculation the molecule is incident on top of an adsorbed rare-gas atom, while in the two-dimensional calculation the molecule is allowed to move in a plane oriented along the [100] direction of the hexagonal adsorbate layer and normal to the surface. These two situations are illustrated in Fig. 2 and will henceforth be referred to as 1D and 2D.

Two extreme situations for the multiple excitation of the Einstein-oscillator modes have been considered in the two-dimensional calculation: in-phase excitations of the Einstein-oscillator modes on all the atoms in the considered plane, and excitations at a single site. We give results for the probabilities $P(n)$ for the excitation of n Einstein-oscillator phonons in the Ar, Kr, and Xe monolayers by the hydrogen molecule. In the 1D calculation for Ar we consider two different incident energies, while in all other calculations we consider only a single energy. We have also calculated the trapping probability at this energy. Only in the 2D situation of single-site multiple phonon excitation will this trapping give rise to sticking. The energy resolution of the incoming wave packet has been chosen to be 1 meV in all cases.

A. Multiphonon distributions: $P(n)$

The results for $P(n)$ in the 1D situation in Fig. 3 show clearly that we have strong multiphonon excitations. The increase of the inelasticity when going from Xe to Kr and to Ar is expected from the fact that the coupling strength is determined by $1/\sqrt{m_a}$ and that both the interaction potentials and the Einstein-oscillator frequencies are similar for these systems. The magnitude of the multiphonon losses and their variation over these systems can be understood semiquantitatively from using the Baule result in a forced-oscillator model.[16–19]

The Baule model is classical and builds on the assumption that the interaction of the particle with the adsorbed atom is impulsive. The result for the energy transfer ΔE
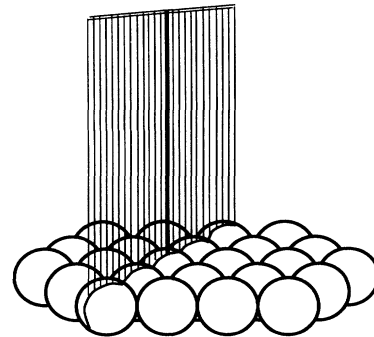

FIG. 2.   The plane in which the 2D calculations are performed is indicated by the stripes. The thick vertical line denotes the path followed in the 1D calculations.

in this model is given by

$$\Delta E = \frac{4\mu}{(1+\mu)^2}(E_i + D),\qquad(33)$$

where $\mu = m_p/m_a$, E_i is the incident energy of the particle, and D is the well depth of the particle-surface potential. We use this result for the energy transfer directly in the forced-oscillator model in order to get a quantum-mechanical multiple phonon loss distribution. In this model such a distribution is obtained by treating the Einstein-oscillator mode quantum mechanically and the particle classically. The force from the particle drives the oscillator and gives rise to multiphonon losses, $P_{\mathrm{FOM}}(n)$, that are distributed according to a Poisson distribution,

$$P_{\mathrm{FOM}}(n) = \exp(-\lambda)\frac{\lambda^n}{n!}.\qquad(34)$$

The intensity λ is the ratio of the definite energy loss, E_{cl}, obtained in a classical description of the oscillator and its vibrational energy ω_E. By equating E_{cl} with
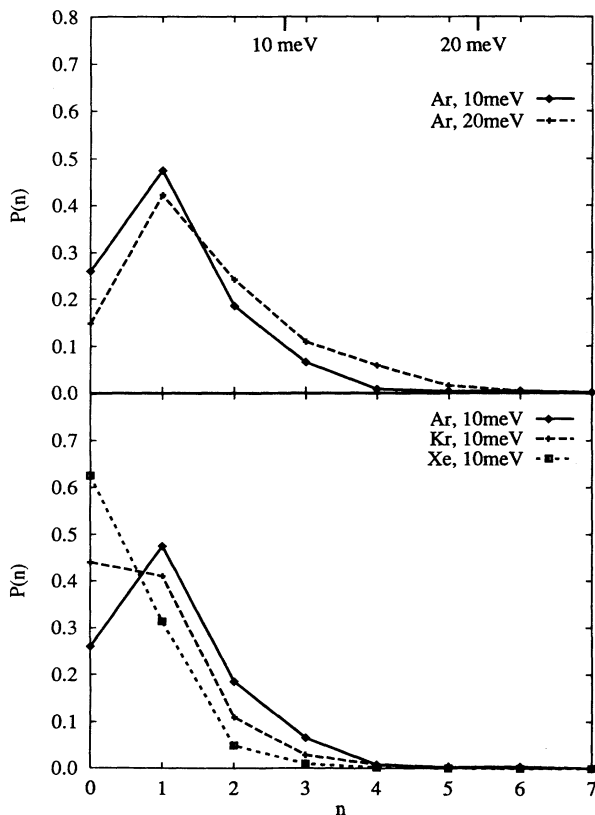

FIG. 3. The probability $P(n)$ for multiphonon excitation as a function of the number n of excited phonons for hydrogen scattered from an overlayer of rare-gas atoms. These calculations are performed in 1D, and the hydrogen molecule comes down on top of a rare-gas atom. (a) When the energy of the molecule incident on an overlayer of argon is increased from 10 to 20 meV, the inelasticity increases. No special effects occur at the vacuum edge, which is marked at the upper edge of the diagram for the two energies, respectively. (b) Larger mass of the rare-gas atom gives decreased inelasticity.

ΔE obtained from the Baule model and using (34), we get the zero-phonon probabilities $P(0)=0.18$, 0.33, and 0.48 at an incident energy of 10 meV. This should be compared with the corresponding probabilities from the one-dimensional calculation, which are 0.26, 0.44, and 0.63 for Ar, Kr, and Xe, respectively. The Baule model thus overestimates the inelasticity, but explains nicely that it increases with decreasing m_a and with increasing incident energy E_i.

We find that if the multiphonon distributions $P(n)$ are compared to Poisson distributions with the same probability for zero-phonon excitation, then the largest deviations occur in the case of strong inelasticity. As can be seen in Fig. 4 the distribution for Xe is close to a Poisson distribution, whereas for Ar at $E_i= 20$ meV the deviations are large.

The combined effects of the strong corrugation and multiphonon excitations of the rare-gas monolayers are investigated in the 2D calculations. The results in Fig. 5 show the probabilities $P(n)$ to excite n Einstein-oscillator phonons. No attempts have been made to make a resolution onto final parallel momenta of the particle leaving the surface, but it can easily be calculated from the k-space distribution of the final wave packet. The upper panel shows the result for $P(n)$ using periodic boundary conditions over the unit cell, which corresponds to an in-phase excitation of the Einstein-oscillator modes in the plane. In the lower panel the periodicity has been broken by introducing absorbing boundary conditions at the edge of the grids. This means that only the atom in the middle cell is excited, which in the limit of an infinite number of unit cells corresponds to a single-site multiphonon approximation. The results from using two and four unit cells, respectively, show that $P(n)$ converges rapidly with the number of cells. In the case of in-phase multiple excitations of the Einstein-oscillator modes the inelasticity decreases compared to the 1D case for all systems, while in the case of single-site multiple excitations
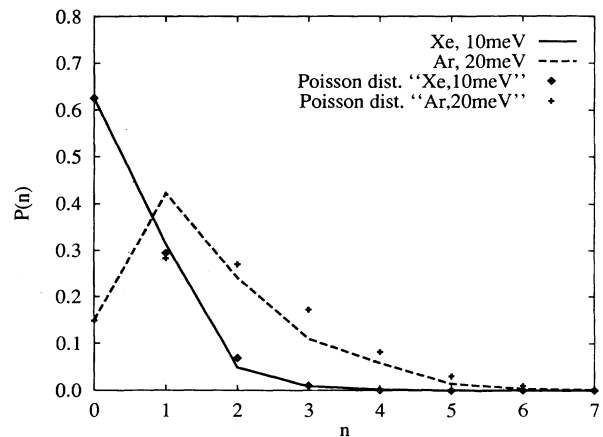

FIG. 4. The probabilities from Fig. 3 (lines) are compared with Poisson distributions (points) with the same probability for zero-phonon excitation. The two extreme cases are shown: scattering from Xe gives almost Poisson distributed multiphonon excitation probabilities; scattering from Ar at 20 meV gives large deviations from a Poisson distribution.
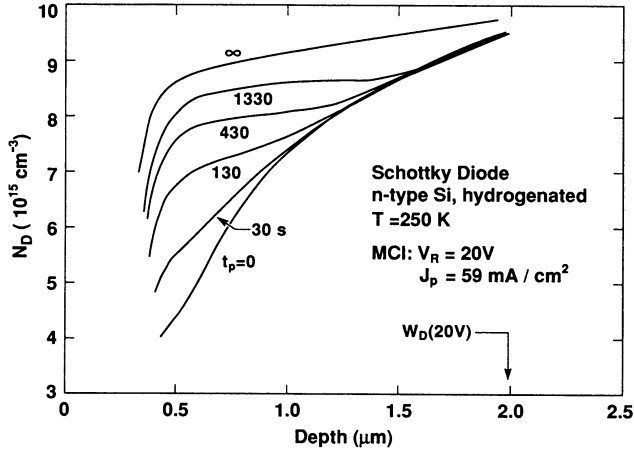
FIG. 2. Depth distributions of the active donor concentration in Schottky diodes on n-type silicon after hydrogenation and after subsequent minority-carrier injections (MCI) at 250 K. Each distribution is labeled with the total elapsed time t_p of MCI. Also shown is the depletion width W_D, corresponding to $V_R = 20$ V during MCI.

depths within the depletion layer there is a rapid recovery of active donors; (2) near the depletion edge W_D, within the space-charge layer, the recovery is greatly suppressed; (3) in the immediate vicinity of the depletion edge there is a detectable *increase* in the PH concentration during the early intervals of hole injection; and (4) after prolonged hole injection (i.e., $t_p \rightarrow \infty$) the donor distribution of the unhydrogenated material is recovered. (The segments of the measured donor profiles nearest the surface are obtained from CV data recorded at or near zero bias, which are subject to the greatest error from the commonly used depletion approximation in the CV analysis; therefore, the donor recovery kinetics were not analyzed at these shallowest depths, as further discussed below.) In the absence of minority-carrier injections (MCI) there was no detectable change in the active donor distribution for the measurement conditions of Fig. 2. When holes were injected under zero bias (i.e., into a charge-neutral region), the time scale of the recovery increased by approximately an order of magnitude, due to significant recapture of H by P in the charge-neutral region, and there was no evidence of a (field-dependent) depth redistribution of PH complexes.

The rapid recovery of active donors at the shallower depths of the space-charge layer, the suppression of the recovery at the greater depths, and the slight increase of the PH concentration at (and immediately beyond) the depletion edge indicate that hole-induced PH dissociation is accompanied by a redistribution of PH complexes within the space-charge layer and that recapture of dissociated hydrogen is greatly reduced at the shallower depths. These observations permit a simplified analysis of the dissociation kinetics. We introduce a phenomenological capture cross section σ_p to describe the interaction between a free hole and a PH complex. For the shallower depths of the space-charge layer we consider only hole-enhanced dissociation of PH complexes with the rate equation

$$\partial n_{PH}(x,t)/\partial t \doteq -\sigma_p v_p p(x) n_{PH}(x,t) , \qquad (1)$$

where n_{PH} is the concentration of PH complexes at a depth x and (elapsed) time t, v_p is the mean thermal velocity of holes, and $p(x)$ is the free-hole concentration at x. Within the space-charge layer, the hole density is obtained directly from the measured hole current:

$$J_p = qp(x)\mu_p E(x) , \qquad (2)$$

where q is electronic charge, μ_p is the hole mobility, and $E(x)$ is the electric-field intensity at depth x. The electric field at any time is readily calculated from the measured active donor profile via Poisson's equation, since the density of mobile charges in the space-charge layer is very small. In the absence of recombination, the solution to Eqs. (1) and (2) yields an exponential decay of n_{PH} with a characteristic time constant

$$\tau_p \equiv q\mu_p E/\sigma_p v_p J_p . \qquad (3)$$

The data were analyzed at the shallower depths (e.g., ~ 0.6 μm in Fig. 2), where the simplifying assumptions were most closely approximated, to obtain the decay time constant, and hence from Eq. (3) the capture cross section, over a range of temperatures. An Arrhenius analysis of σ_p is shown in Fig. 3 and yields an activation energy of ~ 0.3 eV. Note that all of the data were recorded at or below room temperature, where the unassisted thermal dissociation rate is negligible.

The details of the mechanism by which holes accelerate the dissociation of PH complexes remain to be elucidated. As a first step we discuss here the necessary framework for such an elucidation, distinguish the different conceivable mechanisms, and cite some evidence favorable to one mechanism and unfavorable to another.

The dissociation process $PH + h^+ \rightarrow P^+ + H^0$ requires the transformation of the system (Si crystal + P + H), in the space of its nuclear coordinates, from the configuration corresponding to the ground state of PH to that corresponding to widely separated P^+ and H^0, with the hydrogen presumably at a bond-center site. Figure 4(a) illustrates the key features of such a transformation with the ground-state electronic energy of the system $PH + h^+$ plotted versus the P-to-H separation R along
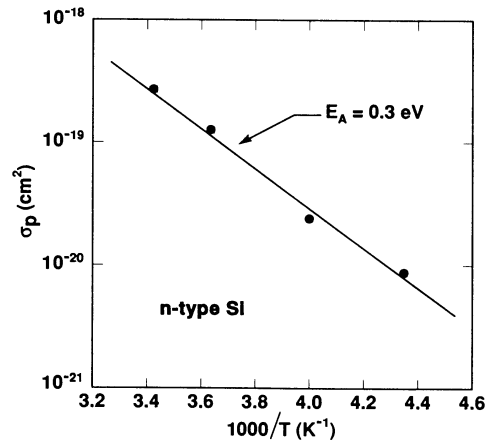

FIG. 3. Arrhenius analysis of the thermally activated cross section for the capture of holes by PH complexes in the space-charge layer of an n-type Schottky diode.

the k-space distribution of each n-phonon amplitude by summing all parts of the amplitude squared having $E_{in} - n\omega_E - K^2/2m < 0$, where K is the momentum parallel to the surface. In 2D this differs from the probability of having the total energy less than zero, as can be seen for the case with periodic boundary conditions in Fig. 6. Just as for the trapping described earlier, we find a separation of time scales for energy loss and gain. The decay of $P_{trap}(t)$ is more rapid in this case than in the total-energy calculations, since some of the particles have a positive total energy and can leave the surface after scattering against the surface corrugation. This trapping probability is found to be large compared to the trapping probability calculated from total energy, around 0.5.

In the single-site calculations much of the amplitudes are absorbed at the edges of the grid during the calculation. If the probability of being absorbed close to the surface is added to the probability of having a perpendicular energy less than zero, the result is close to the corresponding trapping probability in the in-phase excitation, around 0.6 (see Table III).

In the single-site multiphonon approximation trapped particles that have left the single excited oscillator cannot experience any further energy loss to the Einstein-oscillator phonons, they can only scatter from the surface corrugation and will eventually leave the surface again. In reality the trapped particles can continue to lose their energy by exciting Einstein-oscillator phonons. The fate of these particles can be studied in this approximation by considering an initial state where the particle is trapped at the surface with positive energy, and include the possibility for excitation of phonons anywhere at the surface.

IV. SUMMARY

The scattering of light atoms and molecules from rare-gas overlayers is strongly influenced by the large corrugation and shows pronounced inelastic effects, due to vibrational excitation of the rare-gas atoms, which can be described as Einstein oscillators. To describe the possibility of multiphonon excitations of the rare-gas atoms and the corrugation effects at the same time we have proposed a close-coupling wave-packet method, where the wave packets correspond to either single-site multiphonon excitations or in-phase multiphonon excitations of the entire surface layer.

From our calculations in one dimension we find that the scattering is strongly inelastic. The multiphonon distributions show large deviations from Poisson distributions for scattering against argon; for the heavier rare-gas atoms the deviations are smaller. In two dimensions with periodic boundary conditions, corresponding to in-phase multiphonon excitations, the inelasticity is weaker and the probabilities are almost Poisson distributed. For argon we have also used absorbing boundary conditions in the two-dimensional calculations, corresponding to single-site multiphonon excitations. This gives multiphonon distributions close to the one-dimensional ones.

TABLE III. The trapping probability for hydrogen on an overlayer of argon calculated from the criteria of total energy, E_{tot}, or energy for the motion in the z direction, E_z, less than zero. In the calculations over 2 and 4 unit cells, absorbing boundaries are used at the end of the grid close to the surface. The probability for being absorbed there is added to the probability for having $E_z < 0$.

	$E_{tot} < 0$	$E_z < 0$
1D	0.09[a]	
2D, 1 u.c.	0.09[a]	0.50[a]
2D, 2 u.c. abs. bound.	0.06	0.64
2D, 4 u.c. abs. bound.	0.06	0.56

[a]In one dimension and in two dimensions with periodic boundaries the final trapping is always zero, since the initially trapped particles never leave the interaction region. The value given here is the initial trapping, which occurs directly after the first collision with the surface.

In one dimension and in two dimensions with periodic boundary conditions the particle can never leave the region of interaction, and can therefore never stick. The trapping probability in these cases has been calculated as the maximum of the probability to have an energy less than zero as a function of time. The energy transfer from the molecule to the surface is fast compared to the reverse process, meaning that if the particle has a large velocity it will leave the excited oscillator before any energy transfer back to the oscillator has occurred. In this case the scattered hydrogen obviously acquires such a large velocity from the scattering against the surface corrugation; the probabilities for sticking ($E_{tot} < 0$) and trapping ($E_z < 0$ or absorbed close to the surface) in the single-site calculations are very close to the corresponding quantities in the 1D calculation and the 2D calculation with periodic boundary conditions, 0.1 and 0.6, respectively.

Here we have only calculated the distribution on different multiphonon states averaged over all angles. This distribution might vary with scattering angle, so for a direct comparison with experiments momentum-resolved distributions are necessary. These can be calculated directly from the momentum distribution of the final wave packets. To get quantitative agreement with experiments the calculations also have to be extended to three dimensions; this means a considerable increase in the computational effort, but not so large that it should be prohibitive.

ACKNOWLEDGMENTS

*Present address: Department of Physics and Astronomy, Rutgers University, P.O. Box 849, Piscataway, NJ 08855-0849.

[1] H. Schlichting, D. Menzel, T. Brunner, W. Brenig, and J.C. Tully, Phys. Rev. Lett. **60**, 2515 (1988).

[2] S. Andersson, L. Wilzén, M. Persson, and J. Harris, Phys. Rev. B **40**, 8146 (1989).

[3] R. Manson and V. Celli, Surf. Sci. **24**, 495 (1971).

[4] B.F. Mason and B.R. Williams, Phys. Rev. Lett. **46**, 1138 (1981).

[5] K.D. Gibson and S.J. Sibener, Phys. Rev. Lett. **55**, 1514 (1985).

[6] K.D. Gibson and S.J. Sibener, J. Chem. Phys. **88**, 7862 (1988).

[7] K. Kern, R.D. David, R.L. Palmer, and G. Comsa, Phys. Rev. Lett. **56**, 2823 (1986).

[8] K. Kern, P. Zeppenfeld, R.D. David, and G. Comsa, Phys. Rev. B **35**, 886 (1987).

[9] R. Kosloff and C. Cerjan, J. Chem. Phys. **90**, 7556 (1989).

[10] M. D. Stiles, J. W. Wilkins, and M. Persson, Phys. Rev. B **34**, 4490 (1986).

[11] R. C. Mowrey and D. J. Kouri, Chem. Phys. Lett. **119**, 285 (1985).

[12] M.D. Feit, J. A. Fleck, Jr., and A. Steiger, J. Comp. Phys. **47**, 412 (1982).

[13] A. Askar and A. S. Cakmak, J. Chem. Phys. **68**, 2794 (1978).

[14] K.D. Gibson, C. Cerjan, J.C. Light, and S.J. Sibener, J. Chem. Phys. **88**, 7911 (1988).

[15] K. T. Tang and J. P. Toennies, J. Chem. Phys. **74**, 1148 (1981).

[16] W. Brenig, Z. Phys. B **36**, 81 (1979).

[17] H.-D. Meyer, Surf. Sci. **104**, 117 (1981).

[18] R. Brako and D. M. Newns, Surf. Sci. **117**, 42 (1982).

[19] M. Persson and J. Harris, Surf. Sci. **187**, 67 (1987).